



Original Article

# An Infinite Semi-parabolic Asymmetric Quantum Well: Oscillations in the Peltier Coefficient under the Influence of Intense Electromagnetic Waves

Nguyen Thu Huong<sup>1</sup>, Nguyen Quang Son<sup>1,\*</sup>, Nguyen Dinh Nam<sup>2</sup>, Mai Thi Hue<sup>3</sup>

<sup>1</sup>*Air Defence-Air Force Academy, Doai Phuong, Hanoi, Vietnam*

<sup>2</sup>*VNU University of Science, No. 334 Nguyen Trai, Thanh Xuan, Hanoi, Vietnam*

<sup>3</sup>*Hanoi University of Civil Engineering, 55 Giai Phong, Bach Mai, Hanoi, Vietnam*

Received 9<sup>th</sup> November 2025

Revised 29<sup>th</sup> December 2025; Accepted 9<sup>th</sup> April 2026

**Abstract:** This paper presents a detailed theoretical investigation of the Peltier coefficient (PC) in an infinite semi-parabolic asymmetric quantum well (ISPAQW) under the influence of an intense electromagnetic wave (EMW), considering electron-acoustic phonon scattering as the dominant scattering mechanism. By employing the quantum kinetic equation method, we have derived the analytical expressions for the conductivity tensor ( $\sigma_{xx}^{AP}$ ), the thermoelectric tensor ( $\gamma_{xx}^{AP}$ ), and subsequently, the PC. Numerical calculations were performed to scrutinize the complex dependence of the PC on various system parameters, including the magnetic field (B), temperature (T), EMW frequency ( $\Omega$ ), and confinement frequency  $\omega_z$ . The results reveal that the PC exhibits distinct Shubnikov-de Haas (SdH)-like oscillations, originating from the electron-phonon interaction, as the magnetic field varies. Notably, our study demonstrates that external parameters modulate these oscillations in fundamentally different ways: Increasing the temperature T enhances the oscillation amplitude without altering the peak positions (phase). Increasing the EMW frequency  $\Omega$  strongly suppresses the amplitude and concurrently shifts the peaks toward higher magnetic fields. In contrast, increasing the confinement frequency  $\omega_z$  enhances the amplitude while also shifting the peaks to higher magnetic fields. These findings provide crucial insights into the underlying physical mechanisms and the controllability of thermoelectric effects in semiconductor nanostructures.

**Keywords:** Peltier effect, infinite semi-parabolic asymmetric quantum well (ISPAQW), intense electromagnetic wave (EMW), quantum kinetic equation, electron-acoustic phonon scattering, Shubnikov-de Haas oscillation.

\* Corresponding author.

E-mail address: [sonnq@hus.edu.vn](mailto:sonnq@hus.edu.vn)

<https://doi.org/10.25073/2588-1124/vnumap.5095>

## 1. Introduction

In recent decades, thermoelectric effects in low-dimensional semiconductor systems (LDSS), such as quantum wells, quantum wires, and superlattices, have been the subject of intense theoretical and experimental research [1-3]. The quantum confinement of charge carriers in these nanostructures significantly modifies the density of states, which can lead to a substantial enhancement of thermoelectric efficiency, making them promising candidates for solid-state cooling and energy-harvesting applications [4, 5]. Among these nanostructures, asymmetric quantum wells, particularly the infinite semi-parabolic asymmetric quantum well (ISPAQW), have garnered attention as a practical model for describing modern heterostructures like GaAs/AlGaAs [6].

The Peltier effect, which describes the generation or absorption of heat at the junction of two dissimilar materials when an electric current flows through it, is a cornerstone of thermoelectric cooling [5]. Understanding how to control and optimize the Peltier coefficient (PC) is therefore a critical task. The transport properties of LDSS are known to be highly sensitive to external conditions, such as applied magnetic and electric fields, temperature, and the specific confinement potential of the structure [7].

The application of a perpendicular magnetic field (B) imposes Landau quantization on the electron gas, leading to a host of quantum transport phenomena, such as the Shubnikov-de Haas (SdH) oscillations and the magnetophonon resonance (MPR) effect. Furthermore, the presence of an intense electromagnetic wave (EMW), or laser radiation, introduces a highly non-linear and powerful tool for manipulating the system's properties. This external radiation field can fundamentally alter the electron-phonon scattering probabilities, leading to new transport phenomena such as photostimulated and multiphoton processes. Consequently, an EMW can be used as an external "knob" to actively tune and control the thermoelectric coefficients.

To theoretically model these quantum transport phenomena, a rigorous treatment of the dominant scattering mechanisms is essential. In many compound semiconductors, especially at low temperatures, the interaction between electrons and acoustic phonons is a primary scattering process that governs transport coefficients [3, 7].

While various thermoelectric and thermomagnetic effects have been studied in different nanostructures—such as the Peltier effect in superlattices [3] and quantum wires [2]—a detailed theoretical investigation of the Peltier coefficient specifically within an ISPAQW under the combined influence of an EMW and a B-field, driven by electron-acoustic phonon scattering, remains to be fully explored.

In this paper, we aim to fill this gap. We employ the quantum kinetic equation (QKE) method to derive the analytical expressions for the dynamic conductivity tensor ( $\sigma_{xx}$ ), the thermoelectric tensor ( $\gamma_{xx}$ ), and, consequently, the Peltier coefficient (PC). This study focuses on the electron-acoustic phonon scattering mechanism. We perform numerical calculations for a GaAs/AlGaAs ISPAQW to systematically investigate the dependence of the PC on the four key external parameters: the magnetic field (B), temperature (T), EMW frequency ( $\Omega$ ), and the confinement frequency ( $\omega_z$ ). Our results reveal the distinct and often competing ways in which these parameters can be used to control the quantum oscillations of the PC.

This paper is organized as follows: In Section 2, we present the theoretical framework, detailing the model of the ISPAQW and the derivation of the transport tensors using the QKE. In Section 3, we present and discuss the numerical results for the Peltier coefficient. Finally, we provide our conclusions in Section 4.

## 2. Theoretical Framework

### 2.1. Wave Function and Energy Spectrum of Electrons in an Infinite Semi-parabolic Asymmetric Quantum Well Subjected to Perpendicular Electric and Magnetic Fields

In this work, we investigate the transport properties of a two-dimensional electron gas confined in a quantum well heterostructure. The model assumes that the electron motion is quantized along the growth direction (z-axis) due to an infinite semi-parabolic confinement potential  $\mathcal{U}_z = m_e \omega_z^2 z^2 / 2$ , where  $\omega_z$  is the confinement frequency, characterizing the semi-parabolic part. A constant longitudinal electric field  $\mathbf{E}_x = (E_x, 0, 0)$  is applied along the x-direction, while a static magnetic field  $\mathbf{B} = (0, 0, B)$  is imposed along the z-axis to drive the electron transport. Under these conditions, the single-electron Hamiltonian can be expressed as follows [8, 9]:

$$H = \wp + \mathcal{U}_z + eE_x x, \quad (1)$$

with  $\wp = -(\mathbf{p} + e\mathbf{A})^2 / (2m_e)$ ,  $e$  being the electron charge,  $\mathbf{p}$  the momentum operator,  $\mathbf{A} = (0, Bx, 0)$  the vector potential in the Landau gauge,  $m_e = 0.067m_0$  the effective mass of the electron, and  $m_0$  the free electron rest mass.

The electron stationary states in an ISPAQW are obtained through the solution of the time-independent Schrödinger equation [8-10]

$$H\Phi_{n,N,k_y}(\mathbf{r}) = \mathcal{E}_{n,N,k_y} \Phi_{n,N,k_y}(\mathbf{r}). \quad (2)$$

Upon completing the analytical procedure, the energy spectrum and the total wave function are derived in the following form:

$$\mathcal{E}_{n,N,k_y} = \mathcal{E}_n + \hbar\omega_c \left( N + \frac{1}{2} \right) + \hbar v_d k_y - \frac{1}{2} m_e v_d^2, \quad (3)$$

$$\mathcal{E}_n = \hbar\omega_z \left( 2n + \frac{3}{2} \right), \quad (4)$$

$$\Phi_{n,N,k_y}(\mathbf{r}) = \frac{e^{ik_y y}}{\sqrt{L_y}} \Phi_N(x - x_0) \Phi_n(z), \quad (5)$$

$$\Phi_n(z) = \mathcal{A}_n e^{\left( -\frac{z^2}{2\ell_z^2} \right)} z L_n^{\frac{1}{2}} \left( \frac{z^2}{\ell_z^2} \right), \quad (6)$$

$$\Phi_N(x - x_0) = \mathcal{A}_N e^{\left( -\frac{(x-x_0)^2}{2\ell_c^2} \right)} H_N \left( \frac{x - x_0}{\ell_c} \right), \quad (7)$$

Where  $\mathcal{A}_n = \sqrt{\frac{2n!}{\ell_z^3 \Gamma(n + \frac{3}{2})}}$ ,  $\mathcal{A}_N = \sqrt{\frac{1}{2^N N! \ell_c \sqrt{\pi}}}$ . The harmonic oscillator wave functions  $\Phi_N(x - x_0)$  are centered at  $x_0 = \frac{m_e v_d \ell_c^2}{\hbar} - \ell_c^2 k_y$ . The function  $\Phi_n(z)$  describes the quantized electron motion along the confinement direction z. The characteristic confinement and magnetic lengths are  $\ell_z = \sqrt{\frac{\hbar}{m_e \omega_z}}$  and  $\ell_c = \sqrt{\frac{\hbar}{m_e \omega_c}}$ , respectively.  $\Gamma(x)$  is the Gamma function,  $L_n^k(x)$  is the associated Laguerre polynomial,  $H_N(x)$  is the Hermite polynomial of order N; n and N denote the subband quantum number and the Landau level index, respectively;  $\mathbf{k}_y$  and  $L_y$  represent the electron wave vector and the normalized length along the y-direction. The drift velocity is defined as  $v_d = E_x / B$ , while the cyclotron frequency is given by  $\omega_c = eB / m_e$ .

## 2.2. The Peltier Coefficient in Infinite Semi-parabolic Asymmetric Quantum Well under the Influence of a Strong Electromagnetic Wave for the Electron-acoustic Phonon Scattering

In the GaAs/AlGaAs ISPAQW structure, an intense EMW is applied such that the electric field is given by  $\mathbf{E}(t) = (0, E_0 \sin \Omega t, 0)$  along the y-direction ( $E_0$  and  $\Omega$  represent the amplitude and the frequency, respectively), and this field is introduced through the corresponding vector potential  $\mathbf{A}(t) = (0, \frac{E_0 \cos(\Omega t)}{\Omega}, 0)$ . Under these conditions, the Fröhlich Hamiltonian describing the electron–acoustic phonon interaction in the ISPAQW can be written as [10]:

$$\begin{aligned} H &= \sum_{N,n,k_y} \mathcal{E}_{N,n,k_y} \left( \mathbf{k}_y - \frac{e}{\hbar c} \mathbf{A}(t) \right) c_{N,n,k_y}^\dagger c_{N,n,k_y} + \sum_{\mathbf{q}} \hbar \omega_{\mathbf{q}} b_{\mathbf{q}}^\dagger b_{\mathbf{q}} + \\ &+ \sum_{N,N',n,n',k_y,\mathbf{q}} \mathcal{M}_{n,n',N,N'}(\mathbf{q}) c_{N',n',k_y+\mathbf{q}}^\dagger c_{N,n,k_y} (b_{\mathbf{q}} + b_{-\mathbf{q}}^\dagger) \\ &+ \sum_{N,n,k_y} \varphi(\mathbf{q}) c_{N',n',k_y+\mathbf{q}}^\dagger c_{N,n,k_y}, \end{aligned} \quad (8)$$

here, the creation and annihilation processes of electrons (phonons) are represented by the operators  $c_{N,n,k_y}^\dagger$  ( $b_{\mathbf{q}}^\dagger$ ) and  $c_{N,n,k_y}$  ( $b_{\mathbf{q}}$ ), respectively;  $\varphi(\mathbf{q}) = (2\pi i)^3 (\mathbf{F} + \omega_c[\mathbf{q}, \mathbf{h}]) \frac{\partial}{\partial \mathbf{q}} \delta(\mathbf{q})$  is the effective scalar potential of the system with  $\mathbf{F} = e\mathbf{E}_x + \frac{\mathcal{E} - \mathcal{E}_F}{T} \nabla T$ , in which  $\mathbf{q} = (\mathbf{q}_\perp, q_z)$  is the phonon wave vector,  $\mathbf{q}_z$  denoting the component along the confinement direction and  $\mathbf{q}_\perp$  the in-plane component. The unit vector  $\mathbf{h} = \mathbf{B}/B$  indicates the magnetic field direction, while  $\mathcal{E}$  and  $\mathcal{E}_F$  denote the electron and Fermi energies, respectively. The quantity  $\hbar$  stands for the reduced Planck constant.

$$\mathcal{M}_{n,n',N,N'}(\mathbf{q}) = \mathcal{C}_{\mathbf{q}}^{\text{AP}} \mathfrak{S}_{n,n'}(q_z) \mathcal{J}_{N,N'}(q_\perp), \quad (9)$$

where,  $\mathcal{C}_{\mathbf{q}}^{\text{AP}}$  is electron–acoustic phonon interaction constant,  $|\mathcal{C}_{\mathbf{q}}^{\text{AP}}|^2 = \frac{\hbar D^2 q}{2\rho v_s V_0}$  with  $V_0 = L_x L_y L$ ,  $D$ ,  $\rho$ , and  $v_s$  correspond to the normalization volume of the quantum well structure, the acoustic deformation potential, the crystal mass density, and the sound velocity.  $\mathfrak{S}_{n,n'}(q_z)$  and  $\mathcal{J}_{N,N'}(q_\perp)$  are called the electron form factor and the magnetic form factor in an ISPAQW, which defined by

$$\mathfrak{S}_{n,n'}(q_z) = \langle \phi_n(z) | e^{\pm i q_z z} | \phi_{n'}(z) \rangle, \quad (10)$$

$$\begin{aligned} |\mathcal{J}_{N,N'}(q_\perp)|^2 &= |\langle \phi_N(x - x_0) | e^{\pm i q_x x} | \phi_{N'}(x - x_0) \rangle|^2 \\ &= \frac{N! e^{-a}}{N'!} (a)^{N'-N} L_N^{N'-N}(a), \end{aligned} \quad (11)$$

where,  $a = (q_\perp^2 \ell_c^2)/2$ .

With  $\partial f_{N,n,k_y}(t) = \langle c_{N',n',k_y+\mathbf{q}}^\dagger c_{N,n,k_y} \rangle_t$ , the quantum kinetic equation for the electron distribution function is obtained as follows

$$\frac{i\hbar \partial f_{N,n,k_y}(t)}{\partial t} = \langle [c_{N',n',k_y+\mathbf{q}}^\dagger c_{N,n,k_y}, H] \rangle_t, \quad (12)$$

Substituting the Hamiltonian given in Eq. (8) into Eq. (12) and carrying out the corresponding operator manipulations yield the following expression, where the electron–acoustic phonon scattering is considered elastic and the acoustic phonon energy ( $\hbar\omega_{\mathbf{q}}$ ) is therefore neglected [11].

$$\begin{aligned}
 & \frac{\partial f_{N,n,\mathbf{k}_y}}{\partial t} + (\mathbf{F} + \omega_c[\mathbf{k}_y, \mathbf{h}]) \frac{\partial f_{N,n,\mathbf{k}_y}}{\hbar \partial \mathbf{k}_y} = \\
 & = -\frac{2\pi}{\hbar} \sum_{N,n,N',n',\mathbf{q}} |\mathcal{M}_{n,n',N,N'}(\mathbf{q})|^2 \sum_{s=-\infty}^{+\infty} J_s^2(\hbar \mathbf{q}_y) (2N_q + 1) \\
 & \times \left\{ \left[ f_{N',n',\mathbf{k}_y+\mathbf{q}_y} (N_q + 1) - f_{N,n,\mathbf{k}_y} N_q \right] \delta(\mathcal{E}_{n',N'}(\mathbf{k}_y + \mathbf{q}_y) - \mathcal{E}_{n,N}(\mathbf{k}_y) - s\hbar\Omega) \right. \\
 & \left. + \left[ f_{N',n',\mathbf{k}_y-\mathbf{q}_y} N_q - f_{N,n,\mathbf{k}_y} (N_q + 1) \right] \delta(\mathcal{E}_{n',N'}(\mathbf{k}_y - \mathbf{q}_y) - \mathcal{E}_{n,N}(\mathbf{k}_y) - s\hbar\Omega) \right\}, \tag{13}
 \end{aligned}$$

In this expression,  $J_s(x)$  refers to the Bessel function of order  $s$  and argument  $x$ , and  $\hbar = \frac{eE_0}{m_e\Omega^2}$  defines the parameter associated with the laser-induced dressing of the electron states. Furthermore,  $\delta(x)$  stands for the Dirac delta function, and  $N_q$  corresponds to the phonon occupation number in thermal equilibrium, which obeys the Bose–Einstein distribution. By multiplying both sides of Eq. (13) by  $\frac{e\hbar}{m_e} \mathbf{k}_y \delta(\mathcal{E} - \mathcal{E}_{n,N}(\mathbf{k}_y))$  and then summing over  $n, N$ , and  $\mathbf{k}_y$ , we obtain a compact form of the kinetic equation. For simplicity, the analysis is restricted to one-photon absorption and emission processes, which reduces the Bessel function order in Eq. (13) to  $s = 0, \pm 1$ . After these considerations and straightforward algebraic manipulation, Eq. (13) can be rewritten as follows:

$$\frac{\mathfrak{B}(\mathcal{E})}{\tau(\mathcal{E})} + \omega_c[\mathbf{h}, \mathfrak{B}(\mathcal{E})] = \mathfrak{Q}(\mathcal{E}) + \mathfrak{S}(\mathcal{E}), \tag{14}$$

$$\mathfrak{Q}(\mathcal{E}) = -\frac{e\hbar}{m_e} \sum_{N,n,\mathbf{k}_y} \mathbf{k}_y \left( \mathbf{F}, \frac{\partial f_{N,n,\mathbf{k}_y}}{\partial \mathbf{k}_y} \right) \delta(\mathcal{E} - \mathcal{E}_{n,N}(\mathbf{k}_y)), \tag{15}$$

$$\begin{aligned}
 \mathfrak{S}(\mathcal{E}) & = \frac{2\pi e}{m_e} \sum_{N',n'} \sum_{N,n} \sum_{\mathbf{k}_y,\mathbf{q}} |\mathcal{M}_{n,n',N,N'}(\mathbf{q})|^2 N_q \mathbf{k}_y \delta(\mathcal{E} - \mathcal{E}_{n,N}(\mathbf{k}_y)) \times \\
 & \times \left\{ (f_{N',n',\mathbf{k}_y+\mathbf{q}} - f_{N',n',\mathbf{k}_y}) \left[ \left( 1 - \frac{\hbar^2 \mathbf{q}_y^2}{2} \right) \delta(\mathcal{E}_{n',N'}(\mathbf{k}_y + \mathbf{q}_y) - \mathcal{E}_{n,N}(\mathbf{k}_y)) + \right. \right. \\
 & \left. \left. + \frac{\hbar^2 \mathbf{q}_y^2}{4} \delta(\mathcal{E}_{n',N'}(\mathbf{k}_y + \mathbf{q}_y) - \mathcal{E}_{n,N}(\mathbf{k}_y) \pm \hbar\Omega) \right] + \right. \\
 & \left. \left\{ (f_{N',n',\mathbf{k}_y-\mathbf{q}} - f_{N',n',\mathbf{k}_y}) \left[ \left( 1 - \frac{\hbar^2 \mathbf{q}_y^2}{2} \right) \delta(\mathcal{E}_{n',N'}(\mathbf{k}_y - \mathbf{q}_y) - \mathcal{E}_{n,N}(\mathbf{k}_y)) + \right. \right. \right. \\
 & \left. \left. \left. + \frac{\hbar^2 \mathbf{q}_y^2}{4} \delta(\mathcal{E}_{n',N'}(\mathbf{k}_y - \mathbf{q}_y) - \mathcal{E}_{n,N}(\mathbf{k}_y) \pm \hbar\Omega) \right] \right\} \right\}, \tag{16}
 \end{aligned}$$

where,  $\tau(\mathcal{E})$  represents the relaxation time,  $\mathfrak{B}(\mathcal{E})$  stands for the partial contribution to the current density vector at energy  $\mathcal{E}$ .

Upon solving Eq. (13), the following expression is derived:

$$\begin{aligned}
 \mathfrak{B}(\mathcal{E}) & = \frac{\tau(\mathcal{E})}{1 + \omega_c^2 \tau^2(\mathcal{E})} \{ \mathfrak{Q}(\mathcal{E}) + \mathfrak{S}(\mathcal{E}) - \omega_c \tau(\mathcal{E}) [\mathfrak{Q}(\mathcal{E}) + \mathfrak{S}(\mathcal{E})] + \\
 & + \omega_c^2 \tau^2(\mathcal{E}) \mathbf{h}(\mathbf{h}, \mathfrak{Q}(\mathcal{E}) + \mathfrak{S}(\mathcal{E})) \} \tag{17}
 \end{aligned}$$

The total current density is determined from the following expression:

$$\mathbf{j}(t) = \int_0^{+\infty} \mathfrak{B}(\mathcal{E}) d\mathcal{E} = \frac{e\hbar}{m_e} \int_0^{+\infty} \sum_{N,n,\mathbf{k}_y} \mathbf{k}_y f_{N,n,\mathbf{k}_y}(t) \delta(\mathcal{E} - \varepsilon_{n,N}(\mathbf{k}_y)) d\mathcal{E}. \quad (18)$$

Based on the expression for the total current density  $\mathbf{j}$ , the electrical conductivity tensor  $\sigma_{\text{im}}^{\text{AP}}$  and the thermoelectric tensor  $\beta_{\text{im}}^{\text{AP}}$  can be extracted using the thermoelectric transport equation [13],

$$\mathbf{j} = \sigma_{\text{im}}^{\text{AP}} \mathbf{E}_m + \beta_{\text{im}}^{\text{AP}} \nabla \mathbf{T}_m. \quad (19)$$

Subsequently, to determine the analytical forms of the remaining tensors  $\gamma_{\text{im}}^{\text{AP}}$  and  $\xi_{\text{im}}^{\text{AP}}$ , we utilize the thermal flux density relation as outlined in reference [13]

$$\mathfrak{Q}(\mathcal{E}) = -\frac{1}{e} \int_0^{+\infty} (\mathcal{E} - \varepsilon_F) \mathfrak{B}(\mathcal{E}) d\mathcal{E} = \gamma_{\text{im}}^{\text{AP}} \mathbf{E}_m + \xi_{\text{im}}^{\text{AP}} \nabla \mathbf{T}_m. \quad (20)$$

The quantity  $\sigma_{\text{xx}}^{\text{AP}}$  represents the electrical conductivity tensor, while  $\gamma_{\text{xx}}^{\text{AP}}$  describes the dynamic tensor associated with the electric field  $\mathbf{E}_m$ . The analytical expressions for these kinetic tensors are given as follows:

$$\sigma_{\text{xx}}^{\text{AP}} = \frac{\tau(\varepsilon_F)(1 - \omega_c \tau)}{1 + \omega_c^2 \tau^2 (\varepsilon_F)} \wp_0 + (\mathcal{K}_1 + \mathcal{K}_2) \wp_1 + \mathcal{K}_3 \wp_2 + \mathcal{K}_4 \wp_3 \quad (21)$$

$$\gamma_{\text{xx}}^{\text{AP}} = (\mathcal{K}_1 + \mathcal{K}_2)(\Delta_\varepsilon - \varepsilon_F) \wp_1 + \mathcal{K}_3(\Delta_\varepsilon - \hbar\Omega - \varepsilon_F) \wp_2 + \mathcal{K}_4(\Delta_\varepsilon + \hbar\Omega - \varepsilon_F) \wp_3, \quad (22)$$

where,

$$\begin{aligned} \wp_0 &= \frac{eL_y}{2\pi m_e \hbar^2 v_d} \varepsilon_{n,N}(\mathbf{k}_y); & \Delta_\varepsilon &= \varepsilon_{n',N'} - \varepsilon_{n,N} + eE_1 \lambda. \\ \wp_1 &= \frac{e\tau^2(\Delta_\varepsilon)}{m_e[1 + \omega_c^2 \tau^2(\Delta_\varepsilon)]^2}; & \wp_2 &= \frac{e\tau^2(\Delta_\varepsilon - \hbar\Omega)}{m_e[1 + \omega_c^2 \tau^2(\Delta_\varepsilon - \hbar\Omega)]^2} \\ \wp_3 &= \frac{e\tau^2(\Delta_\varepsilon + \hbar\Omega)}{m_e[1 + \omega_c^2 \tau^2(\Delta_\varepsilon + \hbar\Omega)]^2}; & \lambda &= \left( \sqrt{N + \frac{1}{2}} + \sqrt{N + \frac{3}{2}} \right) \frac{\ell_c}{2}; \\ \varepsilon_{n,N}(\mathbf{k}_y) &= \hbar\omega_z \left( 2n + \frac{3}{2} \right) + \hbar\omega_c \left( N + \frac{1}{2} \right) + \hbar v_d k_y - \frac{1}{2} m_e v_d^2; \\ \varepsilon_{n',N'} &= \hbar\omega_z \left( 2n' + \frac{3}{2} \right) + \hbar\omega_c \left( N' + \frac{1}{2} \right) - \frac{1}{2} m_e v_d^2 \\ \varepsilon_{n,N} &= \hbar\omega_z \left( 2n + \frac{3}{2} \right) + \hbar\omega_c \left( N + \frac{1}{2} \right) - \frac{1}{2} m_e v_d^2 \\ \mathcal{K}_1 &= \mathcal{G} \left( 1 - \frac{\hbar^2 \lambda^2}{2\ell_c^2} \right) \left[ 1 + 2 \sum_{l=1}^{\infty} (-1)^l e^{\left( -\frac{2\pi l \alpha}{\hbar\omega_c} \right)} \cos(2\pi l \bar{Q}_1) \right] \\ \mathcal{K}_2 &= \mathcal{G} \frac{\hbar^2 \lambda^2}{4\ell_c^2} \left[ 1 + 2 \sum_{l=1}^{\infty} (-1)^l e^{\left( -\frac{2\pi l \alpha}{\hbar\omega_c} \right)} \cos(2\pi l \bar{Q}_1) \right] \\ \mathcal{K}_3 &= \mathcal{G} \frac{\hbar^2 \lambda^2}{4\ell_c^2} \left[ 1 + 2 \sum_{l=1}^{\infty} (-1)^l e^{\left( -\frac{2\pi l \alpha}{\hbar\omega_c} \right)} \cos(2\pi l \bar{Q}_2) \right] \\ \mathcal{K}_4 &= \mathcal{G} \frac{\hbar^2 \lambda^2}{4\ell_c^2} \left[ 1 + 2 \sum_{l=1}^{\infty} (-1)^l e^{\left( -\frac{2\pi l \alpha}{\hbar\omega_c} \right)} \cos(2\pi l \bar{Q}_3) \right] \end{aligned}$$

$$\begin{aligned} \overline{Q}_1 &= \frac{\mathcal{E}_{n,N} - \mathcal{E}_{n',N'} + eE_1\lambda}{\hbar\omega_c}; & \overline{Q}_2 &= \frac{\mathcal{E}_{n,N} - \mathcal{E}_{n',N'} + eE_1\lambda - \hbar\Omega}{\hbar\omega_c} \\ \overline{Q}_3 &= \frac{\mathcal{E}_{n,N} - \mathcal{E}_{n',N'} + eE_1\lambda + \hbar\Omega}{\hbar\omega_c}; & \alpha &= \frac{\hbar}{\tau}; \\ \mathcal{G} &= \frac{e\eta_0\mathcal{D}^2m_e k_B T L_y L}{8\pi^2\hbar^4\rho v_d v_s^3} \int_{-\infty}^{+\infty} |\mathfrak{S}_{n,n'}(q_z)|^2 \lambda(\mathcal{E}_{n,N} - \mathcal{E}_F) dq_z, \end{aligned}$$

with  $\eta_0$  is the electron's density. Here,  $\mathcal{G}$  represents the squared overlap integral describing the conservation of crystal momentum; The terms  $\mathcal{K}_1, \mathcal{K}_2, \mathcal{K}_3$  and  $\mathcal{K}_4$  result from mathematical manipulations involving the transformations and Poisson's summation formula; The parameter  $\lambda$  is derived from the assumption of an effective phonon momentum, specifically  $\hbar v_d q_y \approx eE_1\lambda$ ; The parameters  $\overline{Q}_1, \overline{Q}_2$  and  $\overline{Q}_3$  emerge from the transformation of the Dirac delta function within the Poisson summation framework [9];  $\wp_1, \wp_2$  and  $\wp_3$  serve as intermediate auxiliary variables to simplify the final tensor expressions. The Peltier coefficient is obtained from the conductivity tensor and the dynamic tensor by the formula

$$PC = \frac{\gamma_{xx}^{AP}}{\sigma_{xx}^{AP}} \quad (23)$$

where  $\sigma_{xx}^{AP}$  and  $\gamma_{xx}^{AP}$  are given by Eq. (21) and Eq. (22).

### 3. Numerical Results and Discussion

To clarify the physical meaning of the derived expressions, the Peltier coefficient (PC) is numerically calculated for GaAs/AlGaAs heterostructures using typical material parameters [14, 15]:  $\mathcal{E} = \mathcal{E}_F = 50meV$ ,  $m_e = 0.067 m_0$  (where  $m_0 = 9.1 \times 10^{-31}$  kg is the mass of a free electron),  $\tau = 10^{-12}$  s,  $v_s = 5220$  ms<sup>-1</sup>,  $e_0 = 1.6 \times 10^{-19}$  C,  $e = 2.07e_0$ , and  $\mathcal{E}_0 = 8.86 \times 10^{-12}$ . In the present calculation, only transitions between the nearest energy levels are considered, whereas contributions from higher-state transitions are neglected. Consequently, the analysis is confined to electron transitions between the lowest subbands,  $n = 0 \rightarrow n' = 1$  and  $N = 0 \rightarrow N' = 1$ .

To investigate the dependence of the Peltier coefficient on external parameters, its behavior as a function of magnetic field and temperature is plotted in Figure 1. Figure 1(a) presents the detailed dependence of the PC on the magnetic field B (from B = 1T to B = 5T) at three discrete temperatures: T1=5K (dark blue dashed curve), T2=10K (burnt orange curve), and T3=15K (olive green curve). The most prominent feature is the appearance of clear quantum oscillations. These oscillations are analogous in nature to the Shubnikov-de Haas (SdH) effect, which originates from Landau quantization as the magnetic field increases. As the magnetic field B increases, the amplitude of these oscillations grows significantly. This behavior of oscillations intensifying with the cyclotron frequency (which is directly proportional to B) is consistent with the findings of Le Thai Hung et al. [3]. In their study on semiconductor superlattices, they also observed distinct Shubnikov-de Haas oscillations where the amplitude grows significantly as the magnetic field increases. A key finding is the effect of temperature: as T increases from 5K to 15K, the oscillation amplitude is also significantly enhanced. Critically, however, the position (phase) of the oscillation peaks and valleys along the B-axis remains unchanged with temperature, indicating that the oscillation phase is independent of temperature within this surveyed range.

Fig. 1(b) provides a continuous, comprehensive overview, rendering the PC as a 3D surface plot against both magnetic field B (1-5 T) and temperature T (5-15 K). This plot visually confirms the

conclusions drawn from Figure 1(a). The "ridges," which represent the oscillation peaks, are clearly observed to run almost perfectly parallel to the T-axis, strongly illustrating the temperature-independence of the oscillation phase. Concurrently, the color mapping of these ridges—transitioning from blue (low values) at low T to yellow and red (high values) at  $T = 15\text{K}$ —convincingly affirms that the oscillation amplitude increases sharply with temperature. The plot also shows the ridges growing taller along the B-axis, confirming the amplitude's dependence on the magnetic field. This complex interplay of parameters is an intrinsic characteristic of quantum thermoelectric transport phenomena in low-dimensional semiconductor systems.

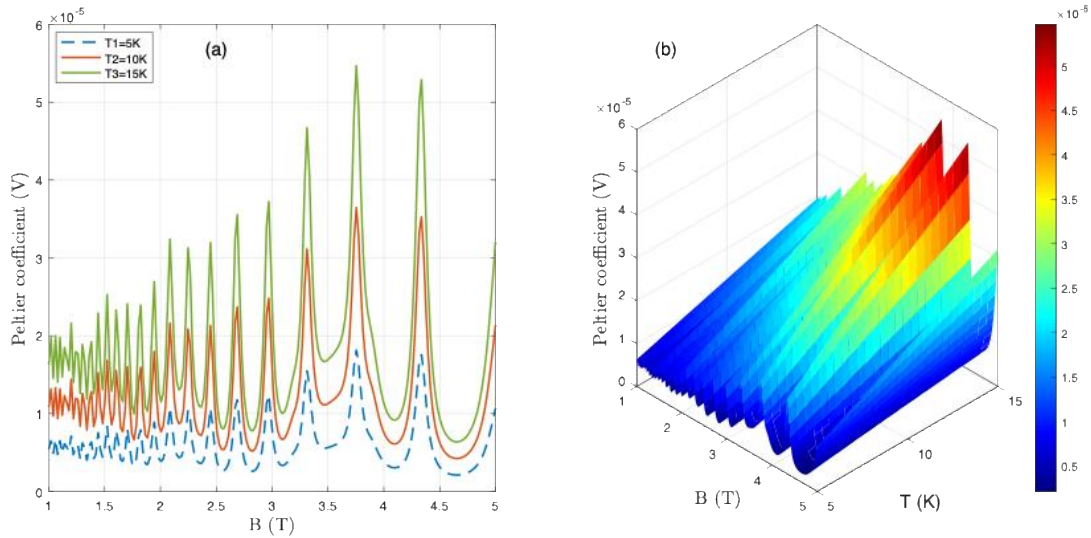


Figure 1. (a) The dependence of the Peltier coefficient on the magnetic field B for three different values of temperature T. (b) The dependence of the Peltier coefficient on the magnetic field B and temperature T.

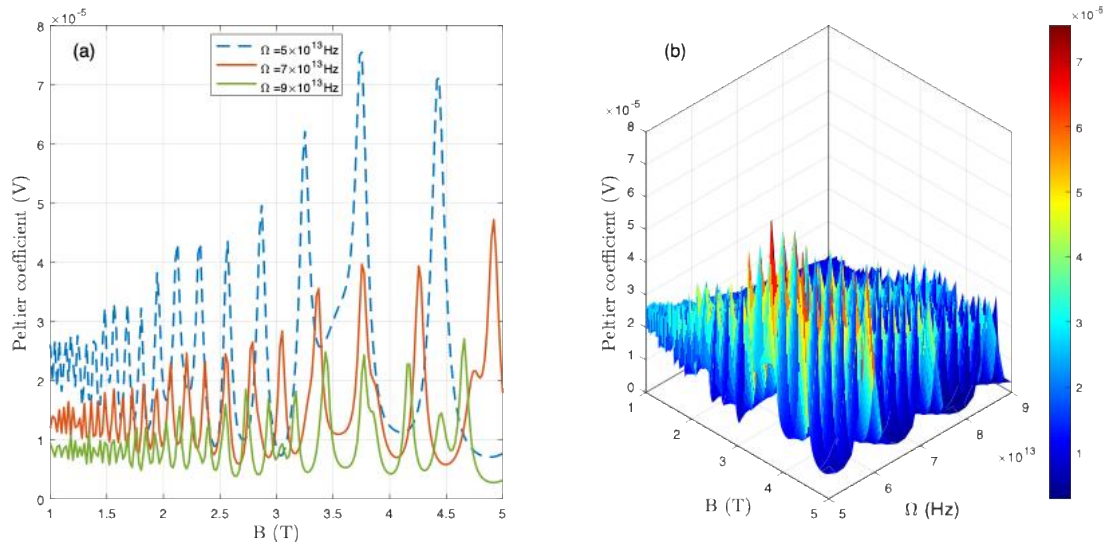


Figure 2. (a) The dependence of the Peltier coefficient on the magnetic field B for three different values of intense EMW frequency  $\Omega$ . (b) The dependence of the Peltier coefficient on the magnetic field B and intense EMW frequency  $\Omega$ .

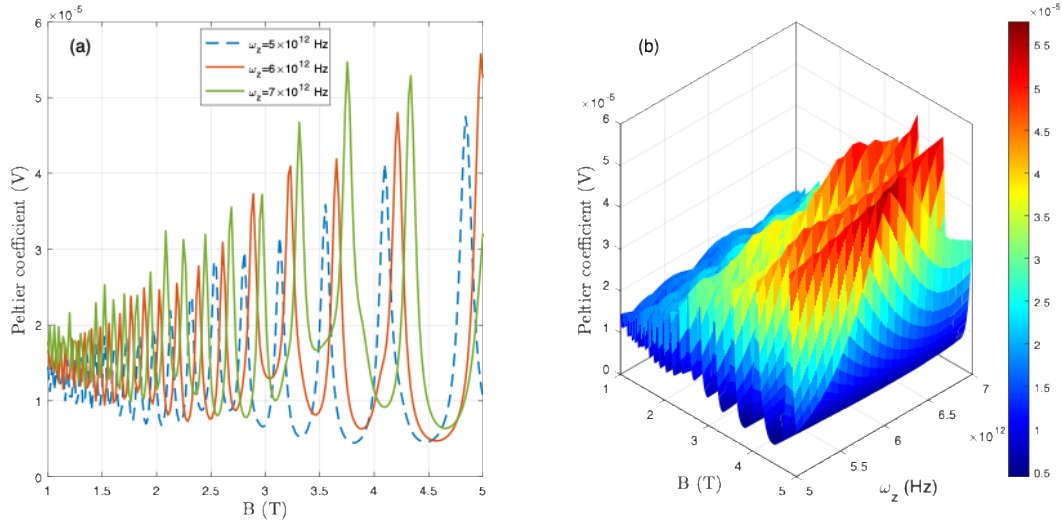


Figure 3. (a) The dependence of the Peltier coefficient on the magnetic field B for three different values of the confinement frequency  $\omega_z$ . (b) The dependence of the Peltier coefficient on the magnetic field B and confinement frequency  $\omega_z$ .

Continuing the investigation, Figure 2 examines the influence of an external high-frequency EMW ( $\Omega$ ) on the PC. Fig. 2(a) displays the PC's dependence on the magnetic field B at three different EMW frequencies:  $\Omega = 5 \times 10^{13}$  Hz (dark blue dashed curve),  $7 \times 10^{13}$  Hz (burnt orange curve), and  $9 \times 10^{13}$  Hz (olive green curve). A stark contrast to the temperature dependence (shown in Fig. 1) is immediately apparent: increasing the frequency  $\Omega$  causes a strong suppression of the oscillation amplitude. The peaks at  $\Omega = 5 \times 10^{13}$  Hz (dark blue dashed curve) are significantly more pronounced than those at  $\Omega = 9 \times 10^{13}$  Hz (olive green curve). Furthermore, a critical feature is that the positions of the resonant peaks clearly shift toward higher magnetic fields as  $\Omega$  increases. This is theoretically consistent, as the magnetophonon resonance (MPR) conditions, which determine the peak locations, are directly dependent on the frequency of the external EMW.

Figure 2(b), a 3D surface plot of the PC versus both B and  $\Omega$ , provides a powerful visualization that confirms the analysis from Figure 2(a). The oscillatory "ridges" are tallest and most defined in the low-frequency region (near  $\Omega = 5 \times 10^{13}$  Hz). As  $\Omega$  increases toward  $\Omega = 9 \times 10^{13}$  Hz, these peaks are rapidly damped, causing the surface to flatten significantly (transitioning to dark blue). In a fundamental departure from Figure 1, these ridges do not run parallel to the  $\Omega$ -axis; instead, they curve and shift, visually demonstrating that the quantum oscillation phase is strongly modulated by the frequency of the EMW.

Next, Figure 3 investigates the effect of the confinement frequency ( $\omega_z$ )—a parameter characterizing the quantum well structure—on the PC. Figure 3(a) illustrates the PC's dependence on the magnetic field B at three different confinement frequencies:  $\omega_z = 5 \times 10^{12}$  Hz (dark blue dashed curve),  $6 \times 10^{12}$  Hz (burnt orange curve), and  $7 \times 10^{12}$  Hz (olive green curve). It is observed that as  $\omega_z$  increases, the amplitude of the quantum oscillation peaks is clearly enhanced. Concurrently, a key feature is that the peak positions shift toward the higher magnetic field region. This shift is a direct consequence of the changing confinement potential;  $\omega_z$  modifies the system's energy structure, which in turn alters the magnetophonon resonance (MPR) condition. Consequently, a stronger magnetic field B is required to satisfy the resonance condition at a higher confinement frequency.

The 3D surface plot in Figure 3(b) illustrates the PC's simultaneous dependence on both  $B$  and  $\omega_z$ , providing a robust visualization of the conclusions from Fig. 3(a). The "ridges" (oscillation peaks) are shown to grow taller and more pronounced as  $\omega_z$  increases from 5 to  $7 \times 10^{12}$  Hz, rather than being suppressed (as seen in Fig. 2). Furthermore, these ridges curve noticeably, shifting to higher  $B$  values as  $\omega_z$  increases (they do not run parallel to the  $\omega_z$ -axis). This confirms that both the amplitude and the phase of the quantum oscillations are strongly modulated by the spatial confinement of the electrons in the quantum well.

#### 4. Conclusion

In this work, we have presented a comprehensive theoretical study of the Peltier coefficient in an infinite semi-parabolic asymmetric quantum well, focusing on the electron-acoustic phonon scattering mechanism. By applying the quantum kinetic equation method, we have successfully derived the analytical expressions for the conductivity tensor ( $\sigma_{xx}^{AP}$ ), the thermoelectric tensor ( $\gamma_{xx}^{AP}$ ), and subsequently, the analytical expression for the Peltier coefficient.

The numerical calculations and discussion have clarified the complex dependence of the PC on system parameters. We have demonstrated that the PC exhibits distinct Shubnikov-de Haas (SdH)-like quantum oscillations as the magnetic field  $B$  varies, which originate from the electron-phonon interaction under Landau quantization. The central finding of this study is the demonstration that these oscillations can be controlled by external factors, but in fundamentally different ways:

- Temperature ( $T$ ): Enhances the oscillation amplitude without altering their phase (peak positions).
- EMW Frequency ( $\Omega$ ): Acts to suppress the oscillations. As  $\Omega$  increases, the amplitude is strongly damped, and the resonant peaks shift toward higher magnetic fields.
- Confinement Frequency ( $\omega_z$ ): Acts to enhance the oscillations. As  $\omega_z$  increases, the amplitude is enhanced, and the resonant peaks also shift toward higher magnetic fields.

These findings provide a clear picture of the physical mechanisms governing quantum thermoelectric effects. They confirm that the thermoelectric transport properties in semiconductor nanostructures can be effectively controlled and tuned (e.g., "switching" oscillations on or off, or optimizing the PC value) by adjusting external factors such as temperature, electromagnetic radiation, and the confinement design of the structure.

#### References

- [1] A. F. Ioffe, L. S. Stil'bans, E. K. Iordanishvili, T. S. Stavitskaya, and A. Gelbtuch, Semiconductor Thermoelements and Thermoelectric Cooling, *Physics Today*, Vol. 12, No. 5, 1959, pp. 42, <https://doi.org/10.1063/1.3060810>.
- [2] T. T. Dien, C. T. V. Ba, N. Q. Bau, N. T. N. Anh, Calculation of Parallel Peltier Coefficient in Rectangular Quantum Wires under the Influence of Confined Optical Phonons and Electromagnetic Waves Using Quantum Kinetic Equation, *Journal of the Korean Physical Society*, Vol. 82, 2023, pp. 1187-1195, <https://doi.org/10.1007/s40042-023-00781-2>.
- [3] L. T. Hung, N. T. L. Quynh, N. T. N. Anh, N. Q. Bau, The Influence of Confined Acoustic Phonon on the Quantum Peltier Effect in Doped Semiconductor Superlattice in the Presence of Electromagnetic Wave, *Journal of Physics: Conference Series*, Vol. 1932, 2021, pp. 012009, <https://doi.org/10.1088/1742-6596/1932/1/012009>.
- [4] Y. G. Gurevich, G. N. Logvinov, *Physics of Thermoelectric Cooling*, *Semiconductor Science and Technology*, Vol. 20, No. 12, 2005, pp. R57, <https://doi.org/10.1088/0268-1242/20/12/R01>.
- [5] Y. G. Gurevich, J. E. V. Pérez, *Peltier Effect in Semiconductors*, (New York: John Wiley and Sons), 2014.

- [6] C. T. V. Ba, N. Q. Bau, N. T. L. Quynh, N. D. Nam, and D. T. Long, Theoretical Study of Photo-stimulated Thermo-magnetolectric Effects in Two-dimensional Compositional Superlattices Using Quantum Kinetic Equation, *Journal of the Korean Physical Society*, Vol. 81, No. 8, 2022, pp. 757-769, <https://doi.org/10.1007/s40042-022-00584-x>.
- [7] N. Q. Bau, D. T. Hang, D. M. Quang, N. T. T. Nhan, Magneto–thermoelectric Effects in Quantum Well in the Presence of Electromagnetic Wave, *VNU Journal of Science: Mathematics–Physics*, Vol. 33, No. 2, 2017, pp. 1-9, <https://doi.org/10.25073/2588-1124/vnumap.4071>.
- [8] P. Vasilopoulos, M. Charbonneau, C. M. Van Vliet, Linear and nonlinear Electrical Conduction In Quasi-Two-Dimensional Quantum Wells, *Physical Review B*, Vol. 35, No. 3, 1987, pp. 1334, [doi.org/10.1103/PhysRevB.35.1334](https://doi.org/10.1103/PhysRevB.35.1334).
- [9] N. T. Huong, N. Q. Bau, C. T. V. Ba, B. T. Dung, N. C. Toan, A. T. Tran, Theoretical Study of Magnetoresistance Oscillations in Semi-parabolic Plus Semi-Inverse Squared Quantum Wells in the Presence of Intense Electromagnetic waves, *Phys. Scr.*, Vol. 100, 2024, pp. 015984.
- [10] N. Q. Bau, N. T. H. Anh, D. V. Toan, N. T. Long, Effect of Electron-Confined Optical Phonon Scattering on the Ettingshausen Effect in GaAs/AlAs Quantum Well With Parabolic Potential Under Laser Radiation, *Commun. Phys.*, Vol. 31, 2021, pp. 101.
- [11] P. Vasilopoulos, Magnetophonon Oscillations in Quasi-two-dimensional Quantum Wells, *Physical Review B*, Vol. 33, 1986, pp. 8587.
- [12] B. V. Paranjape, J. S. Levinger, Theory of the Ettingshausen Effect in Semiconductors, *Phys. Rev.*, Vol. 120, 1960, pp. 437.
- [13] N. Q. Bau, D. T. Hang, D. T. Long, Study of the Quantum Magneto-thermoelectric Effect in the Two-Dimensional Compositional Superlattice GaAs/AlGaAs under the Influence of an Electromagnetic Wave By Using the Quantum Kinetic Equation, *J. Korean Phys. Soc.*, Vol. 75, 2019, pp. 1004-1016.
- [14] B. K. Ridley, *Quantum Processes in Semiconductors*, Pub. Clarendon Press, Add. Oxford, 1993.
- [15] Jasprit Singh, *Physics of Semiconductors and Their Heterostructures*, Pub. McGraw-Hill, Add. Singapore, 1993.